

Response to Referee #2 (acp-2018-1158)

We Thank Reviewer for his/her constructive comments

Responses to the Specific comments

General comments: This paper conducts ensemble air quality modeling of NO₂, CO, and NH₃ over Asia, and evaluates model performance using measurements data in the North China Plain and Pearl River Delta regions. 14 models including 13 regional models and one global model with common emission inventory, meteorological fields, modeling domain, and horizontal resolutions were used for the ensemble modeling. The results show that NO₂ and CO simulations are mostly underestimated and NH₃ modeling mismatches the observed temporal variations. Possible reasons for the model structural uncertainties and recommendations for the future studies are given by the authors. This paper is good in general and within the scope of Atmospheric Chemistry and Physics. I recommend for publication once the concerns expressed below are addressed.

Reply: The authors appreciate the reviewer for his/her constructive and up-to-point comments. We have carefully considered the comments and revised the manuscript accordingly. Please refer to our responses for more details given below.

Comment 1: Although 14 models are required to use standard meteorological field, the configurations of meteorological models may not be identical. The author also needs to list the configurations of each meteorological model as in Table 1. Meanwhile, since the meteorological parameters have large impact on the modeled concentrations, the modeled meteorological fields also need to be validated against observed data.

Reply: Thanks for this important comment. In MICS-Asia III, most of the CTMs used the standard meteorological fields simulated by WRFv3.4.1, except the WRF-Chem models (M7-M10), GEOS-Chem (M13) and RAMS-CMAQ (M14) which used their own meteorological fields. Following the reviewer's suggestion, a new table listing the configurations of the meteorological simulations were added to the supplementary material (*please see table S1 in the supplementary*). Table R1 presents the configurations of the standard meteorological simulation as well as those used in WRF-Chem models (M7–M10). The GEOS-Chem (M13) was driven by the GEOS-5 assimilated meteorological fields from the Goddard Earth Observing System of NASA Global Modeling Assimilation Office, and the RAMS-CMAQ (M14) was driven by the Regional Atmospheric Modeling System (RAMS). For WRF-Chem models, the configurations of their meteorological models were only slightly different from the standard model (Table

R1). For example, M7 used the same parametrization schemes as the standard model in terms of the microphysics, radiation, boundary layer, cumulus physics and surface physics. The other WRF-Chem models differed from the standard model only in one or two parametrization schemes.

Table R1: Meteorological configurations for the standard meteorological field and different WRF-Chem models

No	Microphysics	Longwave radiation	shortwave radiation	Boundary layer	Cumulus physics	surface physics
Standard	Lin et al. scheme	RRTMG scheme	Goddard shortwave scheme	YSU scheme	Grell 3D ensemble scheme	Unified Noah land-surface model
M7	Lin et al. scheme	RRTM scheme	Goddard shortwave	YSU scheme	Grell 3D ensemble scheme	Unified Noah land-surface model
M8	Lin et al. scheme	RRTMG scheme	RRTMG scheme	Mellor-Yamada-Janjic TKE scheme	Grell 3D ensemble scheme	Unified Noah land-surface model
M9	Lin et al. scheme	RRTMG scheme	RRTMG scheme	YSU scheme	Grell 3D ensemble scheme	Unified Noah land-surface model
M10	Goddard Cumulus Ensemble	Goddard longwave scheme	Goddard shortwave scheme	YSU scheme	Grell 3D ensemble scheme	Unified Noah land-surface model

We agree with the reviewer that the meteorological parameters have large impacts on the simulations of atmospheric chemistry. As suggested, we have added the evaluations of the wind speed (u-wind and v-wind), relative humidity (RH) and air temperature (T) simulated by the standard meteorological model in the revised manuscript (*please see lines 139–143 in the revised manuscript and Sect.S1 in the supplementary*). These parameters are all important meteorological factors that influences the simulations of NO₂, CO and NH₃ concentrations. For example, the wind speed determines the transport of species and the air temperature influences the reaction rates of thermal chemical reactions. The relative humidity and temperature also have impacts on the thermodynamic equilibrium of gases and aerosols.

Three-hourly meteorological observations from the Integrated Surface Database (ISD) compiled by the National Oceanic and Atmospheric Administration (NOAA), U.S. (Smith et al., 2011) were used in this study. We focused on the evaluations of meteorological simulations over the North China Plain (NCP) and the Pearl River Delta region with the observation sites used in evaluation shown in Fig.R1. Figure R2 shows the averaged time series of simulated meteorological parameters and observations over the NCP region from January, 2010 to December, 2010 with an interval of three hours. The evaluation statistics, including correlation coefficient (R), mean bias error (MBE) and root of mean square error (RMSE), were summarized in Table R2. It clearly shows that the standard meteorology simulations well captured the main features of the observed meteorological conditions in the NCP region throughout the year with high

correlation coefficient, small biases and low RMSE for all meteorological parameters. Similar results could be obtained from the evaluations of meteorological conditions over the PRD region (fig R3). These results suggested that the standard meteorological simulations can well reproduce the meteorological conditions of the NCP and PRD region.

Table R2: Evaluation metrics of the standard meteorological simulation

	NCP			PRD		
	R	MBE	RMSE	R	MBE	RMSE
temp (°C)	1.00	0.21	1.08	1.00	-0.22	0.71
RH (%)	0.97	-0.16	5.15	0.97	3.42	4.82
u-wind (m/s)	0.91	-0.08	0.63	0.82	-0.20	0.53
v-wind (m/s)	0.93	0.33	0.76	0.93	0.05	0.81

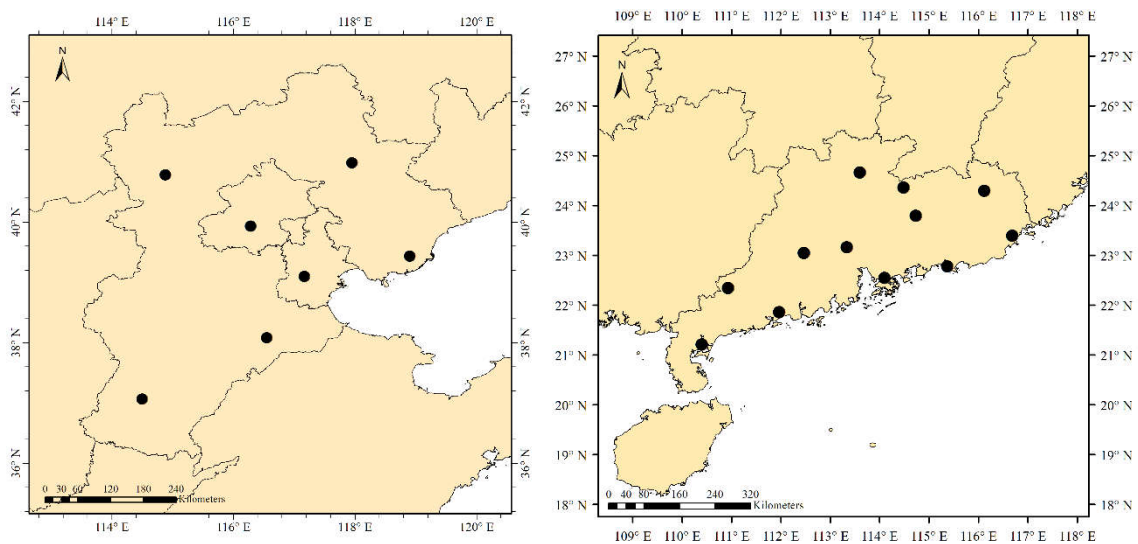


Figure R1: Spatial distributions of the meteorological observation sites from the ISD over the NCP region (left panel) and the PRD region (right panel).

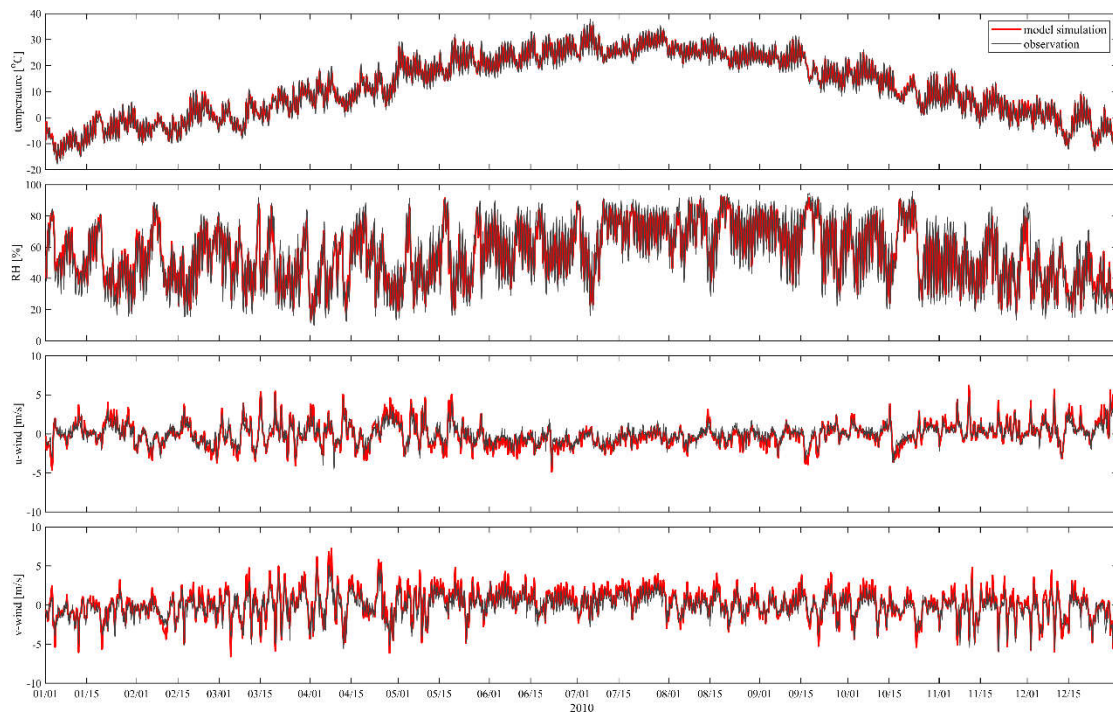


Figure R2: Time series of the simulated and observed meteorological parameters over the NCP region from January 2010 to December 2010 with an interval of three hours.

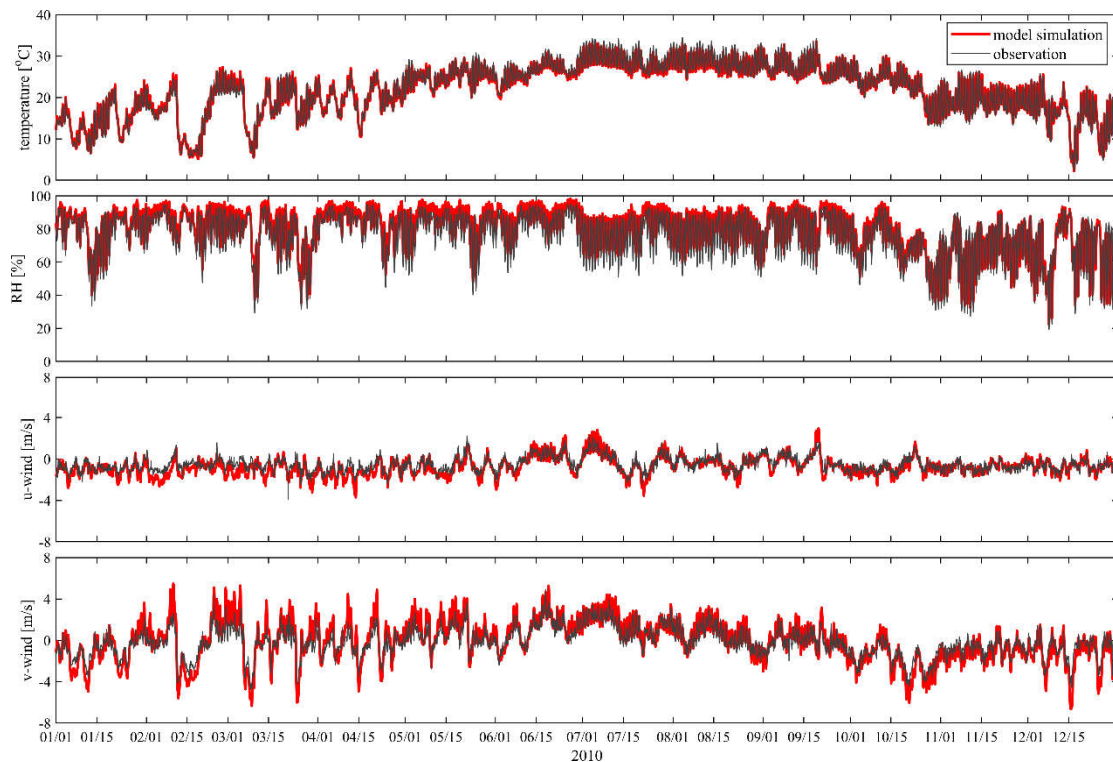


Figure R3: Same as Figure R2 but for the PRD region.

Comment 2: The model performance in PRD is much worse than that in NCP. The author concludes that it is because of coarse horizontal resolution. I think uncertainties may primarily come from the emission

inventory, especially spatial allocations from different emission sectors are not well resolved in the PRD region. I suggest the author use one or two models with finer resolution to test the model performance again in PRD, to see if the horizontal resolution is the main problem as the author demonstrated.

Reply: Thanks for this valuable suggestion. As suggested, a full-year run of NAQPMS model with finer horizontal resolutions has been conducted to investigate the impacts of horizontal resolutions on the simulations of NO₂ and CO over the PRD region. The NAQPMS model is one of the participating CTMs in MICS-Asia III. Two nested domains with finer horizontal resolutions were added to the original modeling domain of MICS-Asia III, which are shown in Fig. R4. The first domain (D1) is identical to the modeling domain of MICS-Asia III with horizontal resolution of 45km; The second domain (D2) covers most part of southeast China with horizontal resolution of 15km; the third domain has the finest horizontal resolution (5km) covering the PRD region and its surrounding areas. The chemical configurations of NAQPMS in each modeling domain were completely identical to those used in MICS-Asia III. Meteorological fields for each modeling domain were simulated by the WRF model version 3.4.1, same as the standard meteorological model in MICS-Asia III. The WRF configurations were also the same as those used in the standard meteorological simulations except two additional nested domains were added (Fig. R4). The emission inventories and boundary conditions in D1 were provided by the standard input datasets of MICS-Asia III. Since MICS-Asia III only provided the emission inventories and boundary conditions at 45km horizontal resolution, in D2 and D3, the emission rates ($\mu\text{g}/\text{m}^2/\text{s}$) and boundary conditions over one model grid were simply obtained from the corresponding model grid in its parent domain. This means that although we used the finer horizontal resolutions in D2 and D3, the resolutions of emission inventories and boundary conditions in D2 and D3 were the same as those used in D1. Therefore, the horizontal resolutions were only dynamically increased in D2 and D3. The simulation results from different modeling domains were then compared with each other to investigate the dynamical impacts of horizontal resolution on the model performance.

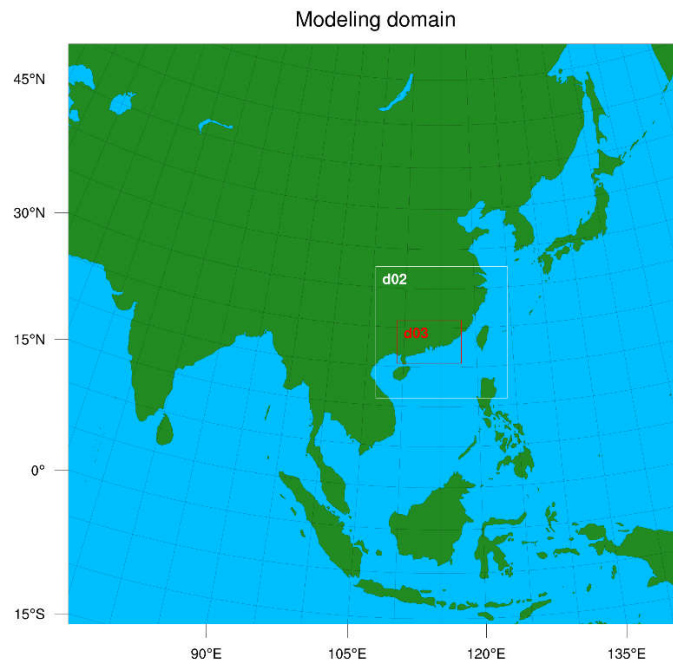


Figure R4: Modeling domain of the sensitivity experiment with different horizontal resolutions.

Figure R5 shows the spatial distributions of the observed annual mean NO_2 concentrations in the PRD region overlay the simulation results using different horizontal resolutions. We can clearly see that the coarse modeling results (D1) cannot resolve the high spatial variability of NO_2 concentrations in the PRD region, which is consistent with what we found from the MICS-Asia III. For simulations using finer horizontal resolutions (D2 and D3), although the spatial scales of NO_2 observations can be resolved by the 15km and 5km resolutions, the modeling results still show poor performance in capturing the observed spatial variability of NO_2 concentrations, with calculated correlation coefficient only of 0.03 and 0.02, respectively (table R2), even worse than the coarse resolutions. Similar results could be obtained from the comparisons of CO observations and simulations with different horizontal resolutions (Fig.R6). These results indicated that the poor model performance in the PRD region may not be attributed to the resolution of model but more related to the resolution and/or spatial allocation of the emission inventories in the PRD region. These results also suggested that only increasing the resolution of the model may not help improve the model performance.

Thus, as the reviewer suggested, the poor model performance in PRD may be more related to coarse resolution and/or inappropriate spatial allocation of the emission inventories in PRD region. Based on these results, we have revised the abstract (*please see lines 43–45 in the revised manuscript*), Section 3.3.1 (*please see lines 244–254 in the revised manuscript*) and Summary (*please see lines 420–424 in the revised manuscript*) part of the manuscript. Analysis of this sensitivity experiments were also added to

the supplementary material (please see Sect.S3 in the supplementary material).

Table R2: Table S3: Evaluation metrics of the simulated annual mean NO₂ and CO concentrations over the PRD region with different horizontal resolutions.

	NO ₂ (ppbv)				CO (ppmv)			
	Spatial R	MBE	NMB (%)	RMSE	Spatial R	MBE	NMB (%)	RMSE
45km	0.09	2.99	13.37	10.53	0.00	-0.51	-52.85	0.57
15km	0.03	2.19	9.81	10.15	0.00	-0.54	-56.25	0.60
5km	0.02	0.58	2.59	10.23	-0.10	-0.57	-59.23	0.62

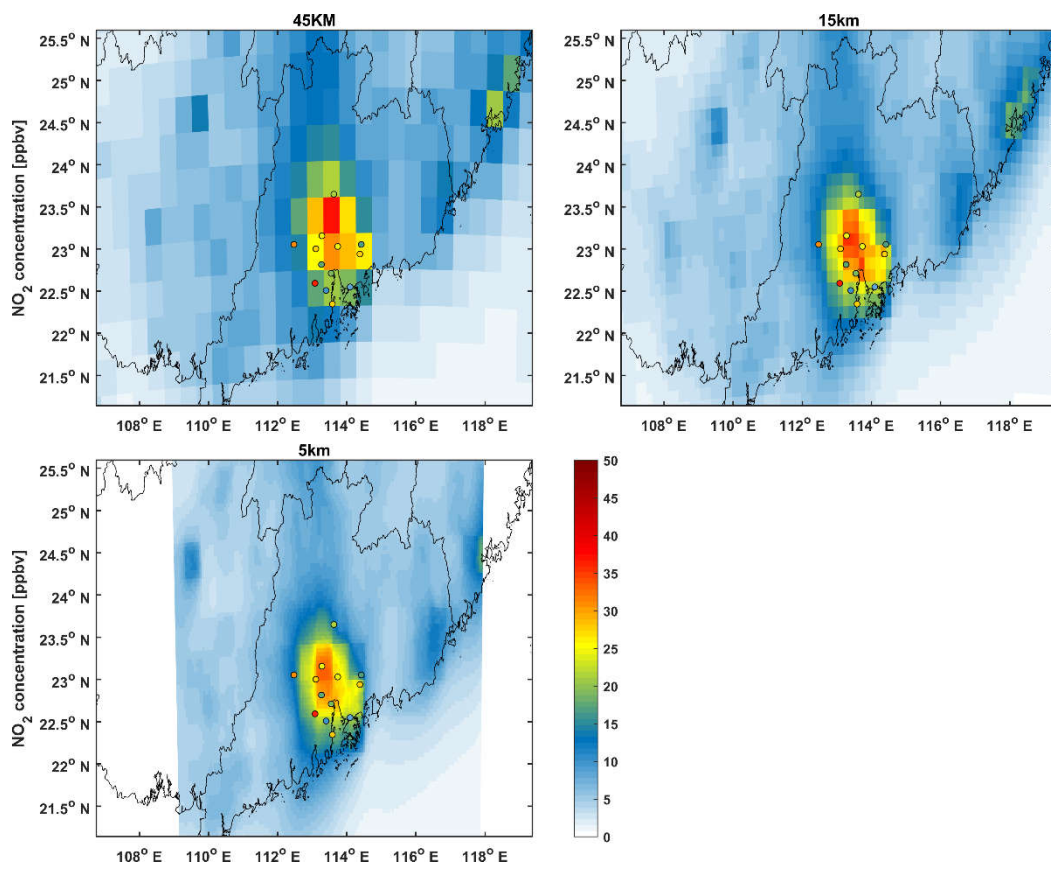


Figure R5: Spatial distributions of the observed and multi-resolution simulated annual mean NO₂ concentrations over the PRD region.

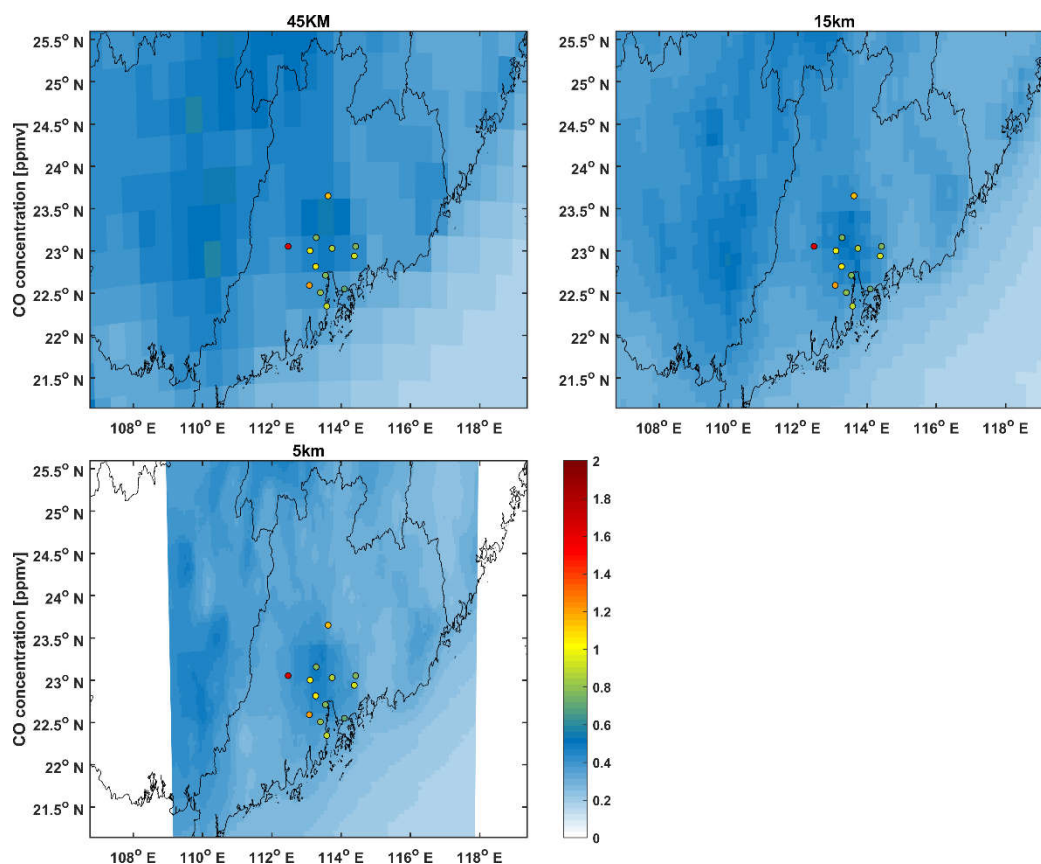


Figure R6: Same as figure R5 but for CO concentrations.

Comment 3: I agreed with the author using the available NH_3 observations from the other years as an alternative to evaluate the performance of different models. However, to evaluate the modeled temporal variations using observed data from different years may not be appropriate, because the NH_3 emissions vary year by year, and control measures may be applied in year of measurement conducted.

Reply: Thanks for this comment. We agree with the reviewer that the use of NH_3 observations from different years may be inappropriate for evaluating the modeled temporal variations due to the emission changes of NH_3 . In the revised manuscript, this problem has been discussed using the satellite retrievals of NH_3 total columns from IASI (Infrared Atmospheric Sounding Interferometer) since we did not obtain the direct surface observations of NH_3 concentration over China in 2010 (*please see lines 202–207 in the revised manuscript*). We used the ANNI-NH3-v2.1R-I retrieval product (Van Damme et al., 2017; Van Damme et al., 2018) in this study which is the reanalysis version of NH_3 retrievals from IASI instruments and provides the daily morning (~9:30 am local time) NH_3 total columns from year 2008 to 2016. The morning orbit was used since IASI is generally more sensitive to the atmospheric boundary layer at this time due to more favorable thermal conditions, which could provide more information on the NH_3 concentrations in the boundary layer where NH_3 is emitted. This dataset was produced by Van Damme et al., 2018 based on the conversion of hyperspectral range indices (HRIs) using an Artificial Neural

Network(Whitburn et al., 2016). It uses the ERA-interim ECWMF meteorological input data rather than the operationally provided EUMETSAT IASI Level 2 (L2) data used for the standard near-real-time version, which is more coherent in time and suitable for the study of temporal variations.

To facilitate comparisons, the NH₃ total columns were averaged to the monthly data at 45km × 45km MICS-Asia grids. A comparison of surface NH₃ observation from AMoN-China and NH₃ total columns from IASI was first conducted to see if IASI measurement could reasonably represent the monthly variations of surface NH₃ concentrations, which is shown in Fig.R7. We can see that the IASI measurement can generally well represent the monthly variations of surface NH₃ concentrations over the NCP region. Both two datasets show a very strong summer peak in July and a subpeak in Spring. However, the IASI NH₃ columns show a steeper monthly variations than the surface NH₃ observations suggested. The month of the subpeak in spring is also different between these two datasets. Nevertheless, the IASI measurement well captured the major monthly patterns of the surface NH₃ concentrations, which can be used to qualitatively evaluate the modeled monthly variations.

Figure R8 shows the spatial distributions of the monthly mean IASI NH₃ total columns over the modeling domain of MICS-Asia III in year 2010. The IASI measurement has a good agreement with the modeled results regarding the spatial distributions of the NH₃ concentrations over East Asia with high columns over Indo-Gangetic Plain and the North China Plain (NCP). However, large discrepancy exists in the monthly variations of NH₃ concentrations over the NCP region between model results and IASI measurements. Consistent with Fig. R7, The IASI NH₃ total columns exhibit significant monthly variations over the NCP region with a strong summer peak in July while the model results shows peak values in November (*Fig.3e in the revised manuscript*). This is consistent with the comparisons of surface NH₃ concentrations, which further confirms the potential deficiency of current CTMs in reproducing the monthly variations of NH₃ concentrations over NCP.

We also plotted the time series of monthly IASI NH₃ total columns averaged over NCP from January, 2008 to December, 2016 to investigate the interannual change of the monthly variations of NH₃ concentrations over NCP, which is shown in Fig. R8. We can see that although there are some interannual changes of magnitude of NH₃ total columns, the monthly pattern of NH₃ total columns is quite similar among different years, which suggests that the interannual change of monthly variation of NH₃ concentrations were very small in these years. Thus, the NH₃ observations from different years could still provide us valuable information on the monthly variation of NH₃ concentrations, which can be used as an alternative to qualitatively evaluate the modeled monthly variation.

These results have been summarized in the revised manuscript (*please see lines 312–323 in the*

revised manuscript) and the supplementary (please see Figure S7-8 in supplementary)

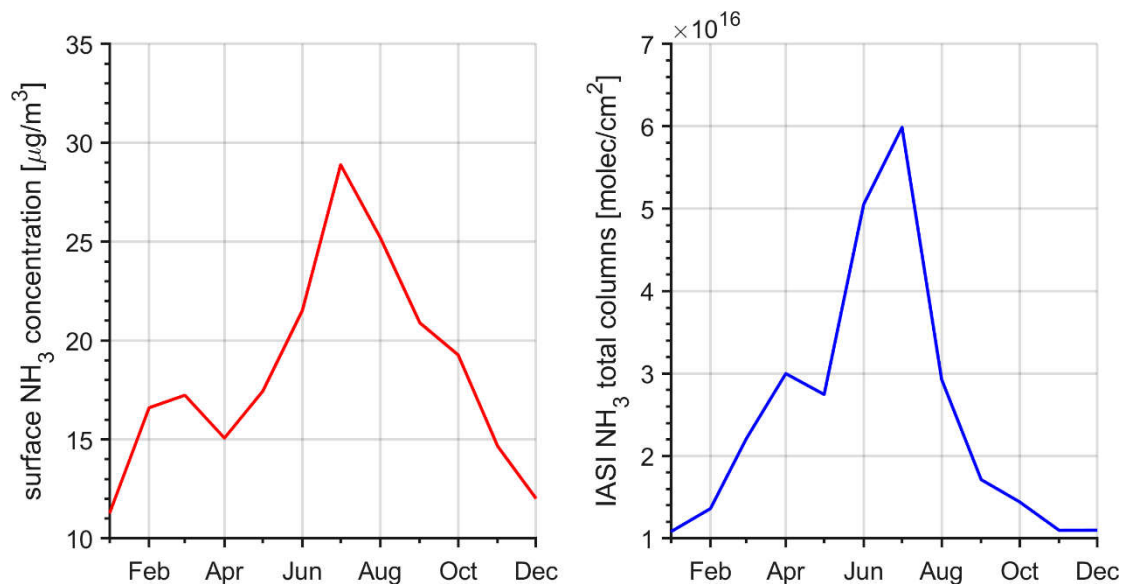


Figure R7: Time series of the surface NH₃ concentrations from AMoN-China (left panel) and NH₃ total columns from IASI (right panel) over the NCP region during September 2015 – August 2016. Note that we reordered the months to better characterize the monthly variations

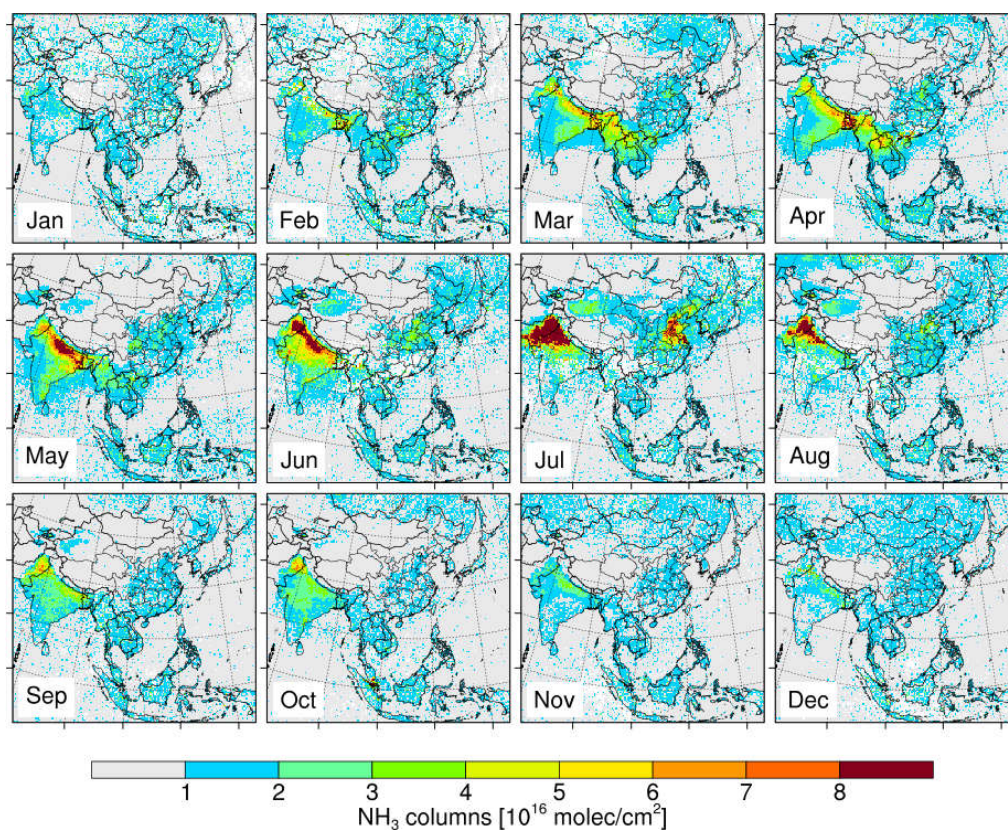


Figure R8: Spatial distributions of the monthly mean IASI NH₃ total columns over the modeling domain of MICS-Asia III

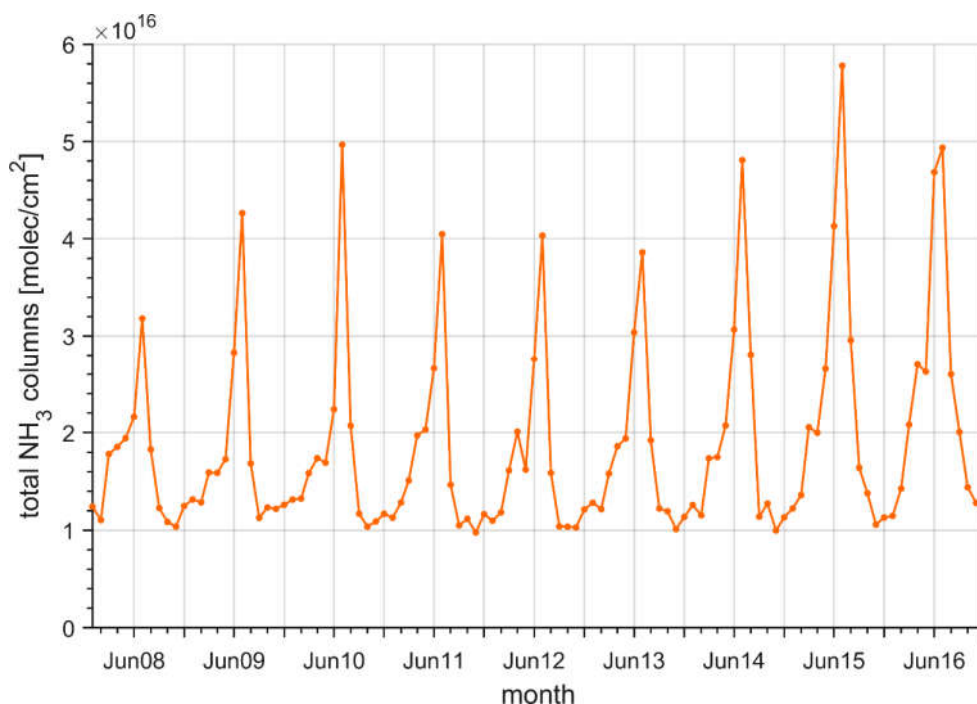


Figure R9: Monthly series of IASI measured NH₃ total columns over the NCP region from year 2008 to 2016.

Comment 4: Figure 5 is an interesting finding in this paper. I am surprised that the NH₃ gas-aerosol partitioning simulations from different models have such large discrepancies. Is it because the chemical mechanisms in different models treating NH₃ different? Otherwise, please explain why does such large discrepancy of NH₃ gas-aerosol partitioning occur in different models.

Reply: Thanks for this comment. As the review mentioned, the gas-chemistry mechanism may contribute to the differences in the modeled gas-aerosol partitioning of NH₃. M9 used the RADM2 mechanism which give lower reaction rates of oxidation of SO₂ and NO₂ by OH radical as compiled by Tan et al., 2019, leading to lower productions of acid and thus lower conversion rate of NH₃ to NH₄⁺. Besides, the hydrolysis of N₂O₅ was not considered in M7, which leads to a lower tendency in the prediction of NO₃⁻ (Chen et al., 2019), and partly explains the higher NH₃ predictions of M7. On the contrary, M14 showed a much lower NH₃/NH_x ratio than most models, which would be related to its higher production rates of sulfate than other models (Chen et al., 2019). For M10, the higher NH₃ predictions of M10 would be related to the inorganic aerosol module used in the model (GOCART). The GOCART aerosol module did not consider the NH₄⁺ aerosol, thus the emitted NH₃ would be only presented as the gas phase in the atmosphere, leading to higher NH₃ predictions in M10. This may also help explain the different monthly variations of NH₃ concentrations seen in M10. Without the considerations of NH₄⁺, the monthly variations of NH₃ concentrations in M10 were more consistent with the monthly variations of NH₃ emissions. This

again highlighted the importance of gas-aerosol partitioning of NH_3 on the predictions of monthly variations of NH_3 concentrations.

Based on these results, we have added more discussions on the potential reasons for the differences in the modeled gas-aerosol partitioning of NH_3 in the revised manuscript (*please see lines 335–339 and lines 343–349 in the revised manuscript*).

Comment 5: In summary, the author makes a few recommendations for future studies. I think inversions of NO_x and CO emissions will help to reduce uncertainties in emission inventory and improve model performance, since many inverse modeling works of NO_x and CO emissions have been done using satellite as well as ground observations. However, I have doubts on inversion of NH_3 because of the reactivity and uncertainties in the chemical pathways of NH_3 gas.

Reply: Thanks for this comment. We agree with the reviewer that the inversion of NH_3 emissions (top-down method) would be more complicated than that for the NO_x and CO emissions due to the larger uncertainties in modeling the atmospheric processes of NH_3 . However, the inversion of NH_3 emissions could still provide valuable clues for verifying bottom-up emission inventories (Zhang et al., 2009) if the models were well validated. In addition, Most of NH_3 is emitted from the non-point sources like livestock or fertilizer uses, which is difficult to be measured over a large domain. As a result, detailed activity data and emission factors for NH_3 emissions are rarely available nationally, leading to high uncertainties in the spatial and temporal patterns of NH_3 emissions. Using the ground or satellite measurements, the top-down methods could give valuable information on the spatial and temporal characteristics of NH_3 emission inventories (Li et al., 2017). Therefore, although there are uncertainties in modeling the processes of NH_3 , several inversion studies has been conducted for NH_3 emissions in U.S., Europe and also China (Gilliland et al., 2003;Paulot et al., 2014;Zhu et al., 2013;Zhang et al., 2018), which has provided valuable suggestions to the improvement of NH_3 emission inventories. Thus, we still believe the top-down methods could help improve the development of NH_3 emissions, however, we have clarified the needs of model validation before the inversion of NH_3 emissions in the revised manuscript (*please see lines 454–461 in the revised manuscript*), which as follows:

“The inversion of NH_3 emissions would be more complicated than the inversion of CO emissions due to the larger uncertainties in modeling the atmospheric processes of NH_3 . Nevertheless, it could still provide valuable clues for verifying the bottom-up emission inventories (Zhang et al., 2009) if the models were well validated. In addition, by using the ground or satellite measurements, the top-down methods could also give valuable information on the spatial and temporal patterns of NH_3 emissions, for example the

inversions studies by (Paulot et al., 2014;Zhang et al., 2018). However, more attention should be paid to the validations of model before the inversion estimation of NH₃ emissions. How to represent the model uncertainties in the current framework of emission inversion is also an important aspect in future studies. Things could be better for CO considering its small and weakly spatial-dependent model uncertainties.”

Other specific comments:

Comment 6: In page 1, line 40, change “peral”to“pearl”.

Reply: We have revised it.

Comment 7: In page 4, line 4, missing “plain”

Reply: We have revised it.

Comment 8: In Figure 1, I think the color of CO measurement sites in NCP should be “green” instead of “blue”.

Reply: We have revised it.

References

- Chen, L., Gao, Y., Zhang, M., Fu, J. S., Zhu, J., Liao, H., Li, J., Huang, K., Ge, B., Wang, X., Lam, Y. F., Lin, C. Y., Itahashi, S., Nagashima, T., Kajino, M., Yamaji, K., Wang, Z., and Kurokawa, J. I.: MICS-Asia III: Multi-model comparison and evaluation of aerosol over East Asia, *Atmos. Chem. Phys. Discuss.*, 2019, 1-54, 10.5194/acp-2018-1346, 2019.
- Gilliland, A. B., Dennis, R. L., Roselle, S. J., and Pierce, T. E.: Seasonal NH₃ emission estimates for the eastern United States based on ammonium wet concentrations and an inverse modeling method, *J. Geophys. Res.-Atmos.*, 108, 12, 10.1029/2002jd003063, 2003.
- Li, M., Liu, H., Geng, G. N., Hong, C. P., Liu, F., Song, Y., Tong, D., Zheng, B., Cui, H. Y., Man, H. Y., Zhang, Q., and He, K. B.: Anthropogenic emission inventories in China: a review, *Natl. Sci. Rev.*, 4, 834-866, 10.1093/nsr/nwx150, 2017.
- Paulot, F., Jacob, D. J., Pinder, R. W., Bash, J. O., Travis, K., and Henze, D. K.: Ammonia emissions in the United States, European Union, and China derived by high-resolution inversion of ammonium wet deposition data: Interpretation with a new agricultural emissions inventory (MASAGE_NH₃), *J. Geophys. Res.-Atmos.*, 119, 4343-4364, 10.1002/2013jd021130, 2014.
- Smith, A., Lott, N., and Vose, R.: The Integrated Surface Database Recent Developments and Partnerships, *Bull. Amer. Meteorol. Soc.*, 92, 704-708, 10.1175/2011bams3015.1, 2011.

- Tan, J., Fu, J. S., Carmichael, G. R., Itahashi, S., Tao, Z., Huang, K., Dong, X., Yamaji, K., Nagashima, T., Wang, X., Liu, Y., Lee, H. J., Lin, C. Y., Ge, B., Kajino, M., Zhu, J., Zhang, M., Hong, L., and Wang, Z.: Why models perform differently on particulate matter over East Asia? – A multi-model intercomparison study for MICS-Asia III, *Atmos. Chem. Phys. Discuss.*, 2019, 1-36, 10.5194/acp-2019-392, 2019.
- Van Damme, M., Whitburn, S., Clarisse, L., Clerbaux, C., Hurtmans, D., and Coheur, P. F.: Version 2 of the IASI NH₃ neural network retrieval algorithm: near-real-time and reanalysed datasets, *Atmos. Meas. Tech.*, 10, 4905-4914, 10.5194/amt-10-4905-2017, 2017.
- Van Damme, M., Clarisse, L., Whitburn, S., Hadji-Lazaro, J., Hurtmans, D., Clerbaux, C., and Coheur, P.-F.: Level 2 dataset and Level 3 oversampled average map of the IASI/Metop-A ammonia (NH₃) morning column measurements (ANNI-NH₃-v2.1R-I) from 2008 to 2016, in, PANGAEA, 2018.
- Whitburn, S., Van Damme, M., Clarisse, L., Bauduin, S., Heald, C. L., Hadji-Lazaro, J., Hurtmans, D., Zondlo, M. A., Clerbaux, C., and Coheur, P. F.: A flexible and robust neural network IASI-NH₃ retrieval algorithm, *J. Geophys. Res.-Atmos.*, 121, 6581-6599, 10.1002/2016jd024828, 2016.
- Zhang, L., Chen, Y. F., Zhao, Y. H., Henze, D. K., Zhu, L. Y., Song, Y., Paulot, F., Liu, X. J., Pan, Y. P., Lin, Y., and Huang, B. X.: Agricultural ammonia emissions in China: reconciling bottom-up and top-down estimates, *Atmos. Chem. Phys.*, 18, 339-355, 10.5194/acp-18-339-2018, 2018.
- Zhang, Q., Streets, D. G., Carmichael, G. R., He, K. B., Huo, H., Kannari, A., Klimont, Z., Park, I. S., Reddy, S., Fu, J. S., Chen, D., Duan, L., Lei, Y., Wang, L. T., and Yao, Z. L.: Asian emissions in 2006 for the NASA INTEX-B mission, *Atmos. Chem. Phys.*, 9, 5131-5153, 10.5194/acp-9-5131-2009, 2009.
- Zhu, L., Henze, D. K., Cady-Pereira, K. E., Shephard, M. W., Luo, M., Pinder, R. W., Bash, J. O., and Jeong, G. R.: Constraining U.S. ammonia emissions using TES remote sensing observations and the GEOS-Chem adjoint model, *J. Geophys. Res.-Atmos.*, 118, 3355-3368, 10.1002/jgrd.50166, 2013.